Catalysis Today 201 (2013) 2–6

Contents lists available at SciVerse ScienceDirect

Catalysis Today

journal homepage: www.elsevier.com/locate/cattod

Activation of solid surface as catalyst

Ken-ichi Tanaka*, Hong He

Research Center for Eco-Environmental Sciences, Chinese Academy of Sciences, Beijing 100085, China

ARTICLE INFO

Article history:
Received 17 January 2012
Received in revised form 25 April 2012
Accepted 7 May 2012
Available online 13 June 2012

Keywords:
Reconstructive activation
Working catalyst surface
Active surface compounds
Structure insensitive catalysis
PROX reaction
NO reduction

ABSTRACT

The original surface of a solid is not always active as a catalyst, but the surface becomes active during reaction. Activation of surfaces may be classified as follows; (i) originally active surfaces, (ii) intermediates produced by reaction with surface atoms, (iii) formation of active sites with functional groups, (iv) formation of active surface compounds, (v) cooperation of multiple catalytic processes. In this review, we discuss two important environmental reactions, one is $NO + H_2 \rightarrow 1/2\ N_2 + H_2O$ catalyzed by single crystal Pt–Rh-ally and Pt/Rh or Rh/Pt bimetals, and the other is the preferential oxidation (PROX) reaction of CO in H_2 by heavily FeO_x-loaded Pt/TiO_2 catalyst and Pt-supported carbon with Ni–MgO. The specific activity of the Pt–Rh catalyst arises from the formation of special ordered bimetallic surface layers composed of (—Rh—O—) on Pt-layer. Formation of an active over-layer compound was confirmed on $Pt_{0.25}Rh_{0.75}$(1 0 0) alloy, Pt/Rh(1 0 0), Rh/Pt(1 0 0), Pt/Rh(1 1 0) and Rh/Pt(1 1 0) bimetal surfaces. The PROX reaction of CO in H_2 was attained on two new catalysts, one being $FeO_x/Pt/TiO_2$ (ca. 100 wt.% FeO_x) and the other Pt supported on carbon with Ni–MgO. The mechanism of the PROX reaction of CO was deduced by in situ DRIFT spectroscopy, which indicates a coupled reaction of $CO + OH^- \rightarrow HCOO^-$ and $HCOO + OH \rightarrow CO_2 + H_2O$.

1. Introduction

This is a review article suggesting a concept for the formation of active surfaces. The surface working as catalyst is sometimes quite different from the original surface, that is, the surface is changed during catalysis. We empirically know that the performance of catalysts is influenced by precursor compounds, support materials, promoting materials, pretreatment temperature, and preheating time, etc. However, the performance of obtained catalysis has been explained in surprisingly primitive ways. That is, activity is explained in relation to the particle size, local bonding structure, coordination atoms and bond length, etc. derived by characterization of catalyst. Catalysis is premised in the conceptional category based on adsorption and reaction. However, the working surface as catalyst is not as simple as supposed, that is, the working surface is different from the original surface but is composed of active materials as has schematically described below (Fig. 1).

As is known, the oxidation of CO with O_2 on Pt is a typical example of category-(i), which was experimentally confirmed by Golchet and White [1]. For catalysis of this category, the activity depends on the kind of metals and the surface. The methanation reaction of CO on Ni, $CO + 3H_2 \rightarrow CH_4 + H_2O$, is a typical catalysis of category-(ii). As demonstrated by Goodman et al. [2], the turn-over frequency for the reaction of $CO + 3H_2 \rightarrow CH_4 + H_2O$ is entirely structure insensitive on various type of Ni-catalysts. This structure-insensitive catalysis was well-rationalized by Tanaka and Hirano [3] as a reaction via the Ni_4C intermediate and it hydrogenation; $4\ Ni + CO + H_2 \rightarrow Ni_4C + H_2O$, $Ni_4C + H_2 \rightarrow CH_2 \rightarrow CH_4^{\bullet} + 4\ Ni$, where the catalysis is caused by recycling of Ni atoms. The ammonia synthesis reaction by Fe-catalyst might be a similar case of catalysis by category-(ii). As Somorjai and his coworkers showed, the ammonia synthesis reaction on Fe single crystal surfaces depends markedly on the crystal planes in a sequence of Fe(1 1 1) ≫ Fe(1 0 0) ≫ Fe(1 1 0) [4,5] They found a dramatic promoting effect of Al_2O_3 on the activity. When Fe(1 1 1), Fe(1 0 0), and Fe(1 1 0) were covered with 2 mL of Al_2O_3 and heated in the presence of H_2O at 723 K, all crystal planes became as active as the Fe(1 1 1) surface [6,7]. Somorjai explained the high activity of Fe(1 1 1) by coordination seven sites denoted as C-7, and the structure-insensitive activity enhanced by Al_2O_3 was also explained by the formation of C-7 sites. However, we propose a different mechanism for such structure-insensitive activity. The reaction of N atom with Fe atom follows a different mechanism, that is, surface Fe atoms react with N atoms to form a reactive Fe_xN intermediate, and its hydrogenation provides ammonia. If this is the mechanism for ammonia synthesis, the reaction might be described by $Fe + 1/2\ N_2 \rightarrow Fe_xN$, $Fe_xN + 3/2H_2 \rightarrow NH_3 + Fe^{\bullet}$, and steady-state reaction is catalyzed by recycling of Fe atoms, which might be increased by loading Al_2O_3. As a result, the activity as catalyst is enhanced by loading Al_2O_3, and the activity becomes structure insensitive.

Catalysis by category-(iii) is similar to that by homogeneous catalysis. A typical example is the hydrogenation of olefins as well as the metathesis reaction of olefins on oxides. For example,

* Corresponding author.
E-mail address: K.Tanaka2012@gmail.com (K.-i. Tanaka).

0920-5861/$ – see front matter © 2012 Elsevier B.V. All rights reserved.
http://dx.doi.org/10.1016/j.cattod.2012.05.007

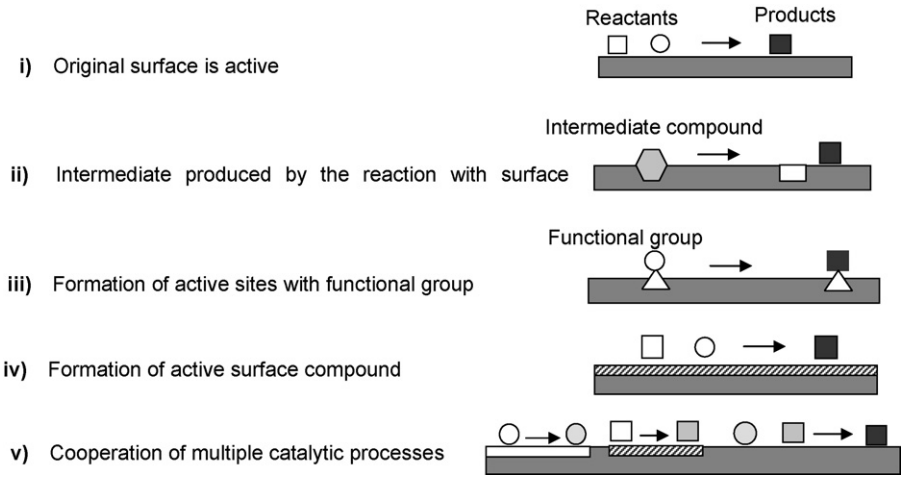

Fig. 1. Activation of surfaces by various processes. Open square and circle indicate reactant, inlayed hexagon in (ii) is intermediate provided by the reaction with surface atom, triangle in (iii) is active sites with functional group, (iv) and (v) are catalysis by forming new active compounds.

sublimated MoO_x (presumably MoO_3) on the inside of a glass tube is entirely inactive, but it changes to a super active catalyst for the olefin metathesis reaction by attaching carbene on Mo sites (Mo = CHR). This surface, however, catalyzes neither the hydrogen scrambling nor the isomerization of olefins, but the olefin metathesis reaction is catalyzed in a stereo-specific manner [8,9]. On the other hand, the catalysis by categories-(iv) and (v) is quite different from homogeneous catalysis. A Pt/Rh three way catalyst activated by category-(iv), and the PROX reaction of CO in H_2 by $FeO_x/Pt/TiO_2$ are discussed in this paper.

2. Formation of active layer for the reduction of NO on Pt–Rh catalyst

The melting temperature of Pt and Rh is very high (nearly 2000 K) so that a clean $Pt_{0.25}Rh_{0.75}(1\,0\,0)$ alloy surface was stable in UHV and no structural and compositional changes occurred up to ca. 1000 K (half of the melting temperature). However, the structure and composition of the Pt–Rh(1 0 0) surface were dramatically changed by raising the temperature in O_2 or in NO to 400–450 K, where a Rh atom was extracted on the topmost surface and the LEED pattern changed from $p(1 \times 1)$ to a unique $p(3 \times 1)$ pattern as shown in Fig. 2(a) [10]. It was confirmed that the Pt–Rh(1 0 0) alloy surface as well as the bimetallic surfaces of Pt-deposited Pt/Rh(1 0 0) and Rh-deposited Rh/Pt(1 0 0) gave the same $p(3 \times 1)$ LEED pattern by raising the temperature in NO or O_2 to 450–600 K. It was also confirmed that the bimetallic surfaces of Rh/Pt(1 1 0) and Pt/Rh(1 1 0) were also readily changed to $p(1 \times 2)$ and $c(2 \times 2)$ structures by raising the temperature in NO or O_2.

The most remarkable feature is that the catalytic activity of the Pt–Rh(1 0 0) alloy and the bimetals of Pt/Rh(1 0 0), Rh/Pt(1 0 0), Rh/Pt(1 1 0), Pt/Rh(1 1 0) gave almost equal catalytic activity for the reaction of $NO + H_2 \rightarrow 1/2\,N_2 + H_2O$ as shown in Fig. 3, although their LEED patterns are $p(3 \times 1)$Pt–Rh(1 0 0)–O, $p(1 \times 2)$Rh/Pt(1 1 0)–O and $c(2 \times 2)$Pt/Rh(1 1 0)–O. That is, Pt–Rh(1 0 0) alloy and Pt/Rh(1 0 0), Pt/Rh(1 1 0), Rh/Pt/(1 0 0) and Rh/Pt(1 1 0) bimetallic surfaces give structure-insensitive high catalytic activity for the reaction of $NO + H_2 \rightarrow 1/2\,N_2 + H_2O$, but the activity of Pt(1 0 0), Pt(1 1 0), Rh(1 0 0) and Rh(1 1 0) surfaces depends markedly on the crystal planes as shown in Fig. 3(a), (b)-1, and (b)-2 [14–17].

The LEED pattern shows different periodic arrays of surface atoms on different crystal planes, but equal catalytic activity suggests the formation of the same compounds on these surfaces. The STM image was attained on a $p(3 \times 1)$ Pt–Rh(1 0 0)–O surface by us [11]. We observed three different STM images for a $p(3 \times 1)$Pt–Rh(1 0 0) surface at different bias potentials. As shown in Fig. 2(b)-ii, two images were observed by an abrupt change of the tip during scanning. Taking these results into account, we derived a structure model of the $p(3 \times 1)$ Pt–Rh(1 0 0)–O surface as shown in Fig. 2. When the $p(3 \times 1)$ Pt–Rh(1 0 0)–O was exposed to O_2 for more than 200 L at 600 K, the LEED pattern changed from the $p(3 \times 1)$ to a $c(2 \times 20)$-hex as shown in Fig. 2(a) [12]. The STM image of the $c(2 \times 20)$-hex Pt–Rh(1 0 0) surface is shown in Fig. 2(c), which shows two slightly rotated compressed domains of (—Rh—O—), which is similar to the STM image with a rotated array of the surface Pt-lattice on a clean (6×20)-Pt(1 0 0)-hex surface. Recently, a similar phenomenon was reported on a FeO_x/Pt(1 1 1) surface [13].

It should be remarked once again that Pt–Rh is a random alloy, but the ordered array of Rh and Pt atoms on the $p(3 \times 1)$ surface made by O_2 is confirmed to be stabilized by the pinning effect of the sub-surface Pt-layer. When the $p(3 \times 1)$ surface is exposed to H_2, the surface quickly changes to the $p(1 \times 1)$ surface at room temperature. The $p(1 \times 1)$ surface was heated in UHV to 600 K and then this $p(1 \times 1)$ surface was exposed to O_2 at room temperature, the $p(3 \times 1)$Pt–Rh(1 0 0) surface was recovered, that is, the ordered array of Pt and Rh atoms was retained at 600 K. The cyclic-voltammogram of the $p(1 \times 1)$ Pt–Rh(1 0 0) surface is very close to that of the Rh(100) surface [14], which is consistent with the proposed model of the $p(3 \times 1)$ surface in Fig. 2.

3. Oxidation of CO and PROX reaction of CO in H_2

Since Langmuir [18] first deduced the mechanism for the oxidation of CO with adsorbed oxygen on Pt surface by kinetics, a large number of studies have been performed on Pt catalysts, and Golchet and White [1] experimentally proved the Langmuir mechanism by measuring CO(a) and O(a) on Pt-foil during catalysis. They showed that the amount of CO(a) and O(a) on the Pt surface during catalysis is given by a dynamic balance of the adsorption and the surface reaction. Therefore, if the P_{CO}/P_{O_2} ratio is changed for constant P_{O_2}, the surface becomes almost clean when the reaction of CO(a) exceeds the adsorption of CO(a), and when higher than this critical ratio of P_{CO}/P_{O_2}, the surface is nearly adsorption equilibrium of CO; whereas when the P_{CO}/P_{O_2} ratio is lower than the critical value, the surface is covered with O(a). This result clearly shows that the oxidation of CO on Pt is catalysis by category-(i).

According to this mechanism, the oxidation of CO in the presence of H_2 on Pt is explained by competitive adsorption and/or competitive reaction of H(a) and CO(a) with O(a). Farrauto and his

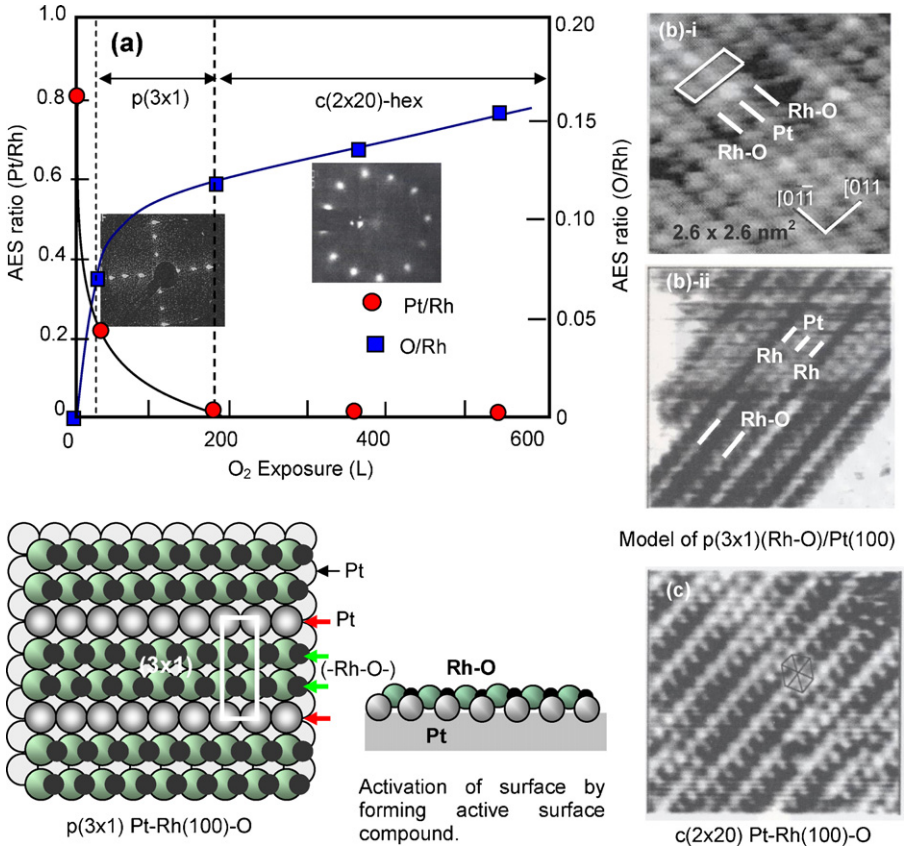

Fig. 2. (a) LEED pattern of $Pt_{0.25}Rh_{0.75}(1\,0\,0)$–O surface changes from $p(1\times1)$ to $p(3\times1)$ and finally $p(2\times20)$-hex by exposure to O_2 at 600 K, (b)-i and (b)-ii are the STM images of a $p(3\times1)$ $Pt_{0.25}Rh_{0.75}(1\,0\,0)$–O surface attained at the same area. In (b-ii) the STM image was abruptly changed. The Pt and (—Rh—O—) were distinctive at different bias potentials, and by abrupt change of the Tip, (c) is the STM image of $c(2\times20)$ surface attained by exposing to O_2 more than 200 L at 600 K. [11].

coworkers [1] found an increase of selectivity for the oxidation of CO in H_2 by adding a small amount of FeO_x (5% in Fe) to a Pt/Al_2O_3 catalyst. They explained this effect of FeO_x as a synergistic effect raising the electron density of Pt; that is, a small amount of FeO_x deposited on Pt weakens the adsorption of CO which results in the enhancement of CO oxidation. Another unusual improved oxidation of CO was reported by Lambert and his coworkers on Pt(1 1 1) surface covered with several monolayers of CeO_2 [19]. The oxidation as well as the adsorption of CO was completely suppressed by one monolayer adsorption of CeO_2 on the Pt(1 1 1) surface as expected, but the oxidation of CO was unexpectedly improved when the Pt surface was covered by more than two layers of CeO_2, although no CO adsorption was observed on this CeO_2/Pt(1 1 1) surface. We speculate that this phenomenon is similar to that observed on Pt-foil when the oxidation reaction exceeds the adsorption of CO(a) at lower than the critical ratio of P_{CO}/P_{O_2} shown by White et al., that is, CeO_2 becomes very active and the oxidation reaction exceeds the adsorption rate of CO on CeO_2/Pt(1 1 1).

Another unusual selective oxidation of CO in H_2 was found by Tanaka et al. [20] on 1 wt% Pt/TiO_2 loaded with a large amount of FeO_x (ca. 100 wt%) ($FeO_x/Pt/TiO_2$). The preferential oxidation (PROX) of CO was attained at low temperature such as 40 °C with very high selectivity. As is discussed in this paper, the oxidation of CO on this $FeO_x/Pt/TiO_2$ catalyst in the presence of H_2 is entirely different from the oxidation of CO on Pt-catalyst given by category-(i) [21,22]. That is, the PROX reaction on $FeO_x/Pt/TiO_2$ is not a competitive reaction of CO(a) and H(a) with O(a).

As shown in Fig. 4(b), the oxidation of CO on FeOx/Pt/TiO_2 was markedly enhanced by H_2 and/or H_2O at 60 °C. In contrast, H_2O and/or H_2 has little effect on the oxidation of CO on 1 wt.% Pt/TiO_2 catalyst as shown in Fig. 4(a) [22]. In addition, the oxidation of CO on the $FeO_x/Pt/TiO_2$ catalyst showed a marked

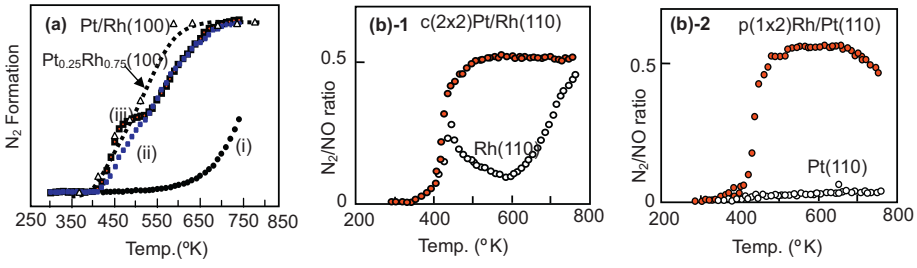

Fig. 3. Catalytic activity of Pt–Rh alloy and bimetal surface for NO (1×10^{-6} Torr) + H_2 (2×10^{-6} Torr) → N_2 reaction. (a) $Pt_{0.25}Rh_{0.75}(1\,0\,0)$ alloy and Pt/Rh(1 0 0) bimetallic surfaces; (i) $p(1\times1)$ Pt/Rh(1 0 0) annealed at 1000 K in UHV, (ii) $p(3\times1)$Pt/Rh(1 0 0) prepared by heating in 1×10^{-7} Torr O_2 at 780 K. (iii) Repeat run of (ii). Broken line shows the activity $Pt_{0.25}Rh_{0.75}(1\,0\,0)$ in a flow of a mixture of 5.8×10^{-9} Torr NO + 1.6×10^{-8} Torr H_2 [14]. (b)-1 NO (1×10^{-6} Torr) + H_2 (2×10^{-6} Torr) → N_2 reaction on Rh(1 1 0) and $c(2\times2)$Pt/Rh(1 1 0) surfaces, and (b)-2 on Pt(1 1 0) and $p(1\times2)$Rh/Pt(1 1 0) [16,17].

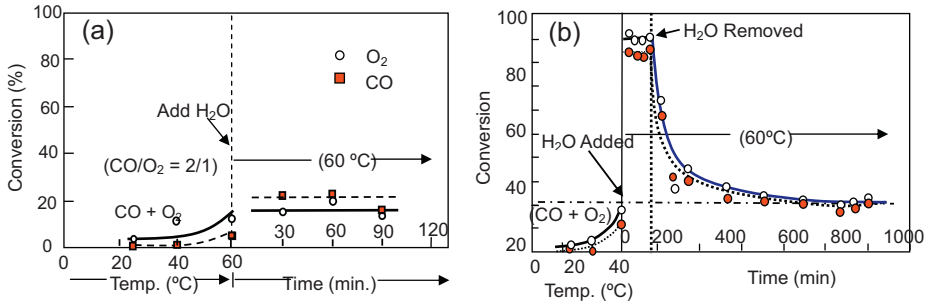

Fig. 4. (a) H_2O has no effect on the oxidation of CO ($CO/O_2 = 1/2$) on a1 wt.% Pt/TiO_2 catalyst at 60 °C. (b) Oxidation of CO on a $FeO_x/Pt/TiO_2$ catalyst at 60 °C is enhanced by adding H_2O to a flow of [CO (3 mL/min) + O_2 (1.5 mL/mi) + N_2 (95.5 mL/min)].

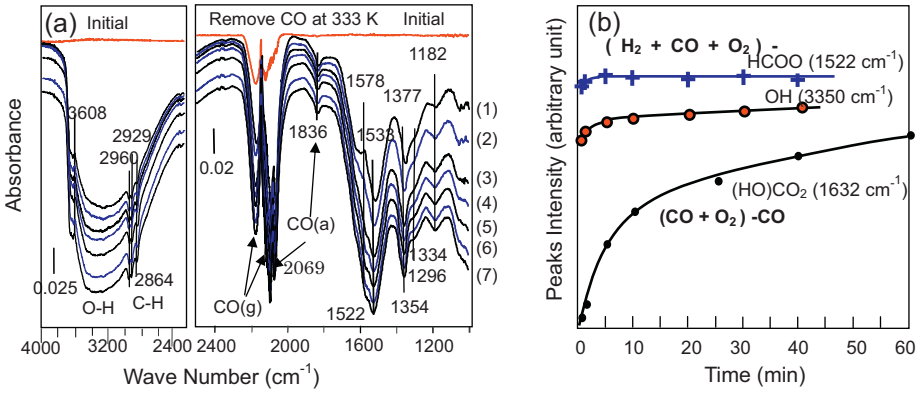

Fig. 5. (a) Change of the in situ DRIFT spectra of $FeO_x/Pt/TiO_2$ with time at 333 K when CO in a flow of $CO + O_2 + H_2$ was stopped [20]. (b) Growth of negative peak intensity is very rapid when the CO flow in a ($CO + O_2 + H_2$) flow was stopped, but the decrease of carbonate peaks in ($CO + O_2$) after stopping CO is slow.

hydrogen isotope effect for the oxidation of CO enhanced by H_2/D_2 or H_2O/D_2O. Therefore, we conclude confidently that the oxidation of CO enhanced by H_2 and/or H_2O on $FeO_x/Pt/TiO_2$ is different from the oxidation of CO(a) with O(a) so far observed on Pt catalysts. The hydrogen isotope effect on the oxidation of CO indicates the involvement of hydrogen atom(s) in the rate determining step of the PROX reaction of CO.

If the PROX reaction of CO proceeds according to the equation $CO(g) \rightarrow CO(a) \rightarrow X(a) \rightarrow CO_2$, and step $X(a) \rightarrow CO_2$ is the rate determining step, and the intermediate X(a) should contain H atom(s). In

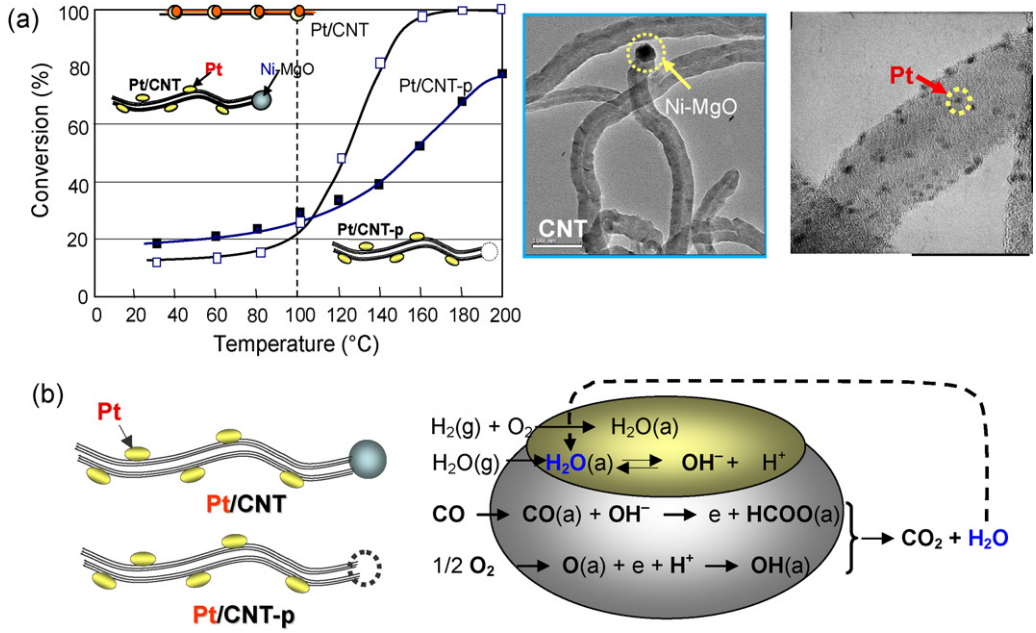

Fig. 6. PROX reaction on Pt/CNT and Pt/CNT-p attained in a flow of CO (1.5 mL/min) + O_2 (1.5 mL/min) + H_2 (15.0 mL/min) + N_2 (42.0 mL/min). (a) Conversion of CO (solid) and of O_2 (open) on 15 wt.%Pt/CNT and 15 wt.%Pt/CNT-p. (0.8 g). CNT; carbon nano-tubes prepared by Ni–MgO, CNT-p; purified Ni–MgO. (b) Proposed reaction schematic for the selective oxidation of CO on $FeO_x/Pt/TiO_2$.

this case, the amount of CO(a) as well as X(a) on the catalyst would be high during steady state of the reaction. Accordingly, when the CO is removed from the gas phase, we could expect a large decrease in the amounts of CO(a) and X(a) according to the reaction rate at the rate determining step.

Based on this idea, in situ DRIFT spectra of the $FeO_x/Pt/TiO_2$ catalyst in a flow of $CO + O_2 + H_2$ were measured by stopping the CO flow in the reactant gas. As shown in Fig. 5(a), a very rapid change in the DRIFT spectra with time was observed at 333 K when the CO was removed from the reactant gas flow. The decreasing rate of CO(a) and X(a) is given by the growth of negative DRIFT peaks, which are obtained by subtracting the steady-state spectrum just before the removal of CO as the background. Therefore, the decrease of intermediates caused by surface reaction or desorption is observed as the growth of negative peaks. The peaks decreasing in Fig. 5(a) are assignable to CO(a) (2069 cm^{-1}), HCOO(a) (1522 cm^{-1}), and OH(a) (3350 cm^{-1}), and the rate of decease of these DRIFT peaks is very rapid as shown in Fig. 5(b) [20]. The DRIFT spectrum of the $FeO_x/Pt/TiO_2$ catalyst in a flow of $CO + O_2$ with no H_2 was entirely different from that attained in a flow of $CO + O_2 + H_2$. That is, the peaks assignable to bi-carbonate decreased slowly at 333 K as shown in Fig. 5(b).

Based on these results, we confidently conclude that the PROX reaction of CO in the presence of H_2 on the $FeO_x/Pt/TiO_2$ catalyst is entirely different from the oxidation of CO with O_2 in the absence of H_2. We suppose that a HCOO intermediate is formed by the reaction of CO with basic OH^- anion on the $FeO_x/Pt/TiO_2$ catalyst in the presence of H_2O. It is worthy of note that formic acid is formed by the reaction of CO with $Ca(OH)_2$, which is an old industrial process. Taking these results into account, we propose a reaction mechanism for the PROX reaction of CO, such as shown in Fig. 6(b) where the oxidation of HCOO(a) takes place by OH(a) instead of O(a).

Recently, we developed new active catalysts for the PROX reaction, which are Pt supported on carbon nanotubes (CNT) and on carbon nano-fiber (CNF). The CNT and CNF employed were prepared using Ni–MgO and Ferrocene as catalysts. Therefore, Pt and Ni–MgO or FeO_x are separated, such that Pt is on the wall but Ni–MgO and FeO_x are localized at the terminal end of the CNT and CNF. Oxidation of CO on the Pt/CNT and Pt/CNF catalysts was markedly enhanced by H_2 and/or H_2O and showed a hydrogen isotope effect [23]. However, if the Ni–MgO and Fe in the nano-tube or nano-fiber were removed by chemical treatment (denoted as CNT-p and CNF-p), the Pt/CNT-p and Pt/CNF were poorly active catalysts for the PROX reaction as shown in Fig. 6(a) [24,25]. The role of Ni–MgO or Fe–Al_2O_3 was confirmed by doping Ni–MgO or Fe–Al_2O_3 onto Pt/graphite and Pt/Vulcan-C. These results suggest that though Pt particles are separated from Ni–MgO, they are indispensable for the PROX reaction catalyst, but the mechanism of enhancement is still unclear [26]. Taking these results into account, we developed an extremely active PROX catalyst for hydrogen fuel cells by doping Ni–MgO onto Pt/Vulcan-C. We succeeded in operating a polymer electrolyte hydrogen fuel cell (PEFC) with H_2 containing 1000 ppm of CO for more than 7 h by installing Pt/Vulcan-C doped with Ni–MgO catalyst at room temperature in the hydrogen fuel line [27].

Acknowledgement

This research was financially supported by the National Natural Science Found for Creative Research Groups of China (No. 50921064).

References

[1] A. Golchet, J.M. White, Journal of Catalysis 53 (1978) 266.
[2] D.W. Goodman, R.D. Kelley, T.E. Madey, J.T. Yates Jr., Journal of Catalysis 63 (1980) 226.
[3] H. Hirano, K.-I. Tanaka, Journal of Catalysis 133 (1992) 461.
[4] S.L. Bernasek, W.L. Siekhaus, G.A. Somorjai, Physical Review Letters 30 (1973) 1202.
[5] N.D. Spencer, C. Schoonmaker, G.A. Somorjai, Journal of Catalysis 74 (1982) 129.
[6] D.R. Strongin, S.R. Bare, G.A. Somorjai, Journal of Catalysis 103 (1987) 289.
[7] D.R. Strongin, J. Carrazza, S.R. Bare, G.A. Somorjai, Journal of Catalysis 103 (1987) 213.
[8] M. Kazuta, K.-I. Tanaka, Journal of the Chemical Society, Chemical Communications (1987) 616.
[9] K. Tanaka, K.-I. Tanaka, H. Takeo, M. Chi, Journal of the American Chemical Society 109 (1987) 2422.
[10] H. Hirano, T. Yamada, K.-I. Tanaka, J. Siera, B.E. Nieuwenhuys, Vacuum 41 (1990) 134.
[11] Y. Matsumoto, Y. Okawa, T. Fujita, K.-I. Tanaka, Surface Science 355 (1996) 109.
[12] T. Matsumoto, Y. Aibara, K. Mukai, K. Moriwaki, Y. Okawa, B.E. Nieuwenhuys, K.-I. Tanaka, Surface Science 377/379 (1997) 32.
[13] Y.-N. Sun, L. Giordano, J. Goniakowski, M. Lewandowski, Z.-H. Qin, C. Noguera, S. Shaikhutdinov, G. Pacchioni, H.-J. Freund, Angewandte Chemie 122 (2010) 4520.
[14] H. Tamura, K.-I. Tanaka, Langmuir 10 (1994) 4530.
[15] A. Sasahara, H. Tamura, K-I. Tanaka, Journal of Physical Chemistry 100 (1996) 15229.
[16] A. Sasahara, H. Tamura, K-I. Tanaka, Catalysis Letters 28 (1994) 161.
[17] A. Sasahara, H. Tamura, K-I. Tanaka, Journal of Physical Chemistry B 101 (1997) 1186.
[18] I. Langmuir, Transactions of the Faraday Society 17 (1921) 607.
[19] C. Hardacre, R.M. Ormerod, R.M. Lambert, The Journal of Physical Chemistry 98 (1994) 10901.
[20] M. Shou, K. Tanaka, K. Yoshioka, Y. Moro-oka, S. Nagano, Catalysis Today 90 (2004) 255.
[21] K.-I. Tanaka, et al., Catalysis Letters 92 (2004) 115.
[22] K.-I. Tanaka, M. Shou, H. He, X. Shi, X. Zhang, Journal of Physical Chemistry C 113 (2009) 12427.
[23] K.-I. Tanaka, M. Shou, H. Zhang, Y. Yuan, T. Hagiwara, A. Fukuoka, J. Nakamura, D. Lu, Catalysis Letters 126 (2008) 89.
[24] K.-I. Tanaka, M. Shou, Y. Yuan, Journal of Physical Chemistry C 114 (2010) 16917.
[25] K.-I. Tanaka, H. He, M. Shou, X. Shi, Catalysis Today 175 (2011) 467.
[26] H. Yang, C. Wang, B. Li, H. Lin, K.-I. Tanaka, Y. Yuan, Applied Catalysis A: General 402 (2011) 168.
[27] K.-I. Tanaka, M. Shou, H. He, C.-G. Zhang, D. Lu, Catalysis Letters 127 (2009) 148.